THE JOURNAL OF BIOLOGICAL CHEMISTRY VOL. 280, NO. 52, pp. 42919–42928, December 30, 2005

Crystallographic Trapping of the Glutamyl-CoA Thioester Intermediate of Family I CoA Transferases*

Received for publication, September 26, 2005, and in revised form, October 21, 2005 Published, JBC Papers in Press, October 27, 2005, DOI 10.1074/jbc.M510522200

Erumbi S. Rangarajan[‡§], Yunge Li[§¶], Eunice Ajamian[‡§], Pietro Iannuzzi[§¶], Stephanie D. Kernaghan[‖], Marie E. Fraser[‖1], Miroslaw Cygler[‡§¶2], and Allan Matte[§¶3]

From the [‡]Department of Biochemistry, McGill University, the [§]Montreal Joint Center for Structural Biology, [¶]Biotechnology Research Institute, National Research Council of Canada, Montreal, Quebec H4P 2R2 and the [‖]Department of Biological Sciences, University of Calgary, Calgary, Alberta T2N 1N4, Canada

Coenzyme A transferases are involved in a broad range of biochemical processes in both prokaryotes and eukaryotes, and exhibit a diverse range of substrate specificities. The YdiF protein from *Escherichia coli* O157:H7 is an acyl-CoA transferase of unknown physiological function, and belongs to a large sequence family of CoA transferases, present in bacteria to humans, which utilize oxoacids as acceptors. *In vitro* measurements showed that YdiF displays enzymatic activity with short-chain acyl-CoAs. The crystal structures of YdiF and its complex with CoA, the first co-crystal structure for any Family I CoA transferase, have been determined and refined at 1.9 and 2.0 Å resolution, respectively. YdiF is organized into tetramers, with each monomer having an open α/β structure characteristic of Family I CoA transferases. Co-crystallization of YdiF with a variety of CoA thioesters in the absence of acceptor carboxylic acid resulted in trapping a covalent γ-glutamyl-CoA thioester intermediate. The CoA binds within a well defined pocket at the N- and C-terminal domain interface, but makes contact only with the C-terminal domain. The structure of the YdiF complex provides a basis for understanding the different catalytic steps in the reaction of Family I CoA transferases.

Coenzyme A is a cofactor utilized by as many as 4% of all enzymes for a diverse variety of biological functions, including cell-cell-mediated recognition, nerve impulse conductance, transcription, and fatty acid biosynthesis and degradation (1, 2). Mainly, these reactions involve the binding and transfer of an acyl group from one substrate to another as part of an enzymatic reaction; it has been noted that coenzyme A is the most prominent acyl group carrier in all living systems (3). Enzyme-catalyzed reactions employing CoA thioesters can be divided into two categories, (i) those where the thioester carbonyl C atom reacts as an electrophile and (ii) those where the thioester α-carbon is deprotonated and reacts as a nucleophile, in Claisen enzymes (1). CoA transferases, which catalyze the reversible transfer of CoA from a donor CoA thioester to a carboxylic acid acceptor generating the free donor and a new acyl-CoA (Scheme 1), belong to the first category of enzymes. Among the large number of CoA transferases, much attention has focused on mitochondrial succinyl-CoA:3-oxoacid CoA-transferase (SCOT),[4] as its autosomal recessive deficiency in humans results in improper ketone body utilization causing episodic severe ketosis, hypoglycemia, and ultimately coma (4, 5).

Three classes of CoA transferases have been defined based mainly on mechanistic and sequence criteria (6). Family I enzymes employ as acceptors 3-oxoacids, short-chain fatty acids, or glutaconate. These enzymes operate with a ping-pong kinetic mechanism and form a covalent thioester intermediate (7). The most thoroughly studied member of the Family I CoA transferases is SCOT. Family II consists of the multifunctional enzymes citrate or citramalate lyase, and unlike Family I enzymes, they do not form a covalent thioester intermediate. Family III enzymes have been discovered more recently, and are distinct both mechanistically (6, 8) and structurally (9) from Family I enzymes. Family III enzymes require formation of an enzyme-substrate ternary complex for catalysis. Both Families I and III of CoA transferases are expected to form either glutamyl- (Family I; Ref. 10) or aspartyl- (Family III; Ref. 8) anhydride intermediates with substrate during the catalytic cycle.

A wealth of biochemical and mechanistic data are available for SCOT, largely based on the pioneering studies of Jencks and collaborators (7, 11–13). These studies established a landmark for the concept of substrate binding energy utilization by an enzyme to effect catalysis, showing that SCOT utilizes its covalent (γ-glutamyl-CoA thioester) and noncovalent interactions with the CoA moiety of the acyl-CoA substrate differentially to reduce the Gibbs activation energy required for catalysis (13). The utilization of this binding energy for catalysis differs for different chemical moieties within the CoA cofactor, as well for the different steps along the reaction coordinate. Although crystal structures are available for three Family I CoA transferases, including glutaconate CoA transferase (GCT) from *Acidaminococcus fermentens* (14), acetate-CoA transferase (ACT, α-subunit) from *Escherichia coli* (15), and SCOT from pig heart (16, 17), no structure has yet been determined with bound substrate or product. The absence of an enzyme-substrate co-crystal structure for any Family I CoA transferase has prevented a detailed understanding of the catalytic mechanism at the atomic level.

Here, we present the crystal structure of YdiF and its complex with CoA, belonging to Family I of the CoA transferases. Activity measurements *in vitro* confirmed that YdiF is indeed a CoA transferase and identified it as having broad substrate specificity for short-chain acyl-CoA thioesters with the activity decreasing when the length of the carboxylic acid chain exceeds four carbons. Co-crystallization with differ-

* This work was supported in part by Canadian Institutes of Health Research Grant 200103GSP-90094-GMX-CFAA-19924. The costs of publication of this article were defrayed in part by the payment of page charges. This article must therefore be hereby marked "*advertisement*" in accordance with 18 U.S.C. Section 1734 solely to indicate this fact.

The atomic coordinates and structure factors (codes 2AHU (apo-YdiF), 2AHV and 2AHW (YdiF-γ-glutamyl-CoA thioester), respectively) have been deposited in the Protein Data Bank, Research Collaboratory for Structural Bioinformatics, Rutgers University, New Brunswick, NJ (http://www.rcsb.org/).

[1] Supported in part by Canadian Institutes of Health Research Grant MOP-42446 and a Biomedical Scholar of the Alberta Heritage Foundation for Medical Research.

[2] To whom correspondence may be addressed. Tel.: 514-496-6321; Fax: 514-496-5143; E-mail: mirek.cygler@nrc-cnrc.gc.ca.

[3] To whom correspondence may be addressed: Biotechnology Research Institute, 6100 Royalmount Ave., Montreal, Quebec H4P 2R2, Canada. Tel.: 514-496-2557; E-mail: allan.matte@nrc-cnrc.gc.ca.

[4] The abbreviations used are: SCOT, succinyl-CoA:3-oxoacid CoA-transferase; GCT, glutaconate CoA transferase; r.m.s., root mean square.

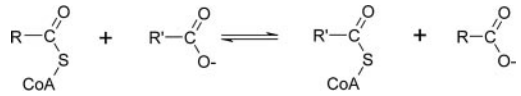

SCHEME 1. **General reaction catalyzed by CoA transferases.** *R* and *R′* refer to the donor and acceptor acyl groups exchanged in the reaction, respectively.

ent CoA derivatives in the absence of an acceptor co-substrate allowed us to capture the structure of the γ-glutamyl-CoA thioester, a reaction intermediate. This structure allows us to propose roles for structurally conserved residues involved in substrate binding or catalysis. Based on the native and γ-glutamyl-CoA thioester crystal structures, we propose a structural description for the steps in the Family I CoA-transferase catalytic cycle.

MATERIALS AND METHODS

Cloning, Expression, and Purification—The *ydiF* gene was amplified by PCR from *E. coli* O157:H7 genomic DNA (18) using *Pfu* polymerase (Stratagene) and oligonucleotide primers (IDT, Coralville, IA). The *ydiF* gene was cloned into a modified pET15b vector (Amersham Biosciences) and expressed in *E. coli* BL21(DE3) as a fusion with a TEV protease-cleavable N-terminal $(His)_8$ tag. The *E. coli* methionine auxotroph strain DL41(DE3) was transformed by the plasmid, for the production of selenomethionine-labeled protein (19).

Bacterial cultures were grown in Circle Grow medium (Qbiogene, Irvine, CA), or LeMaster medium for selenomethionine-labeled protein (19). Protein expression was induced with 100 μM isopropyl 1-thio-β-D-galactopyranoside followed by a 6-h incubation at room temperature. Cell pellets were lysed by solubilization in buffer (50 mM Tris-HCl, pH 8, 0.4 M NaCl, 20 mM imidazole, 5% (v/v) glycerol, 10 mM β-mercaptoethanol, 0.7 mg lysozyme, 10 units/ml Benzonase nuclease (Novagen), 1× Bugbuster detergent solution (Novagen), and 1 tablet of Complete EDTA-free protease inhibitor mixture (Roche Diagnostics). The lysate was clarified by ultracentrifugation (100,000 × *g*, 40 min, 4 °C) and soluble protein was incubated with 2 ml of DEAE-Sepharose (Amersham Biosciences) equilibrated in lysis buffer without lysozyme, Benzonase, or detergent. The flow-through fraction was then loaded onto 2-ml (bed volume) of nickel-nitrilotriacetic acid resin (Qiagen), and washed with 50 mM Tris-HCl buffer (pH 8), 0.4 M NaCl, 5% (v/v) glycerol, 40 mM imidazole, and 10 mM β-mercaptoethanol. YdiF was eluted with the above buffer containing 200 mM imidazole. The eluted protein in 50 mM Tris-HCl buffer (pH 8), 0.4 M NaCl, 5% (v/v) glycerol, and 5 mM dithiothreitol, was concentrated by ultrafiltration to 8 mg/ml. The $(His)_8$ tag was not removed following purification. Selenomethionine-labeled protein was purified in a similar manner.

Gel filtration chromatography was carried out using a Superose 12 HR10/30 column on an Akta Purifier FPLC system (Amersham Biosciences). Purified YdiF enzyme (200 μg) was applied to the column pre-equilibrated with buffer (20 mM Tris-HCl, pH 8, 0.4 M NaCl, 5% (v/v) glycerol, 5 mM dithiothreitol) and protein elution was monitored by UV absorption at λ = 280 nm. Molecular masses were estimated by comparison with the elution profile of molecular mass standards (Sigma). Dynamic light-scattering measurements were done on a DynaPro plate reader molecular sizing instrument (Protein Solutions, Charlottesville, VA) at room temperature using a protein concentration of 8 mg/ml in 20 mM Tris-HCl buffer (pH 8), 0.4 M NaCl, 5% (v/v) glycerol, and 5 mM dithiothreitol.

Mass Spectrometry—Electron spray ionization-mass spectrometry was performed using an Agilent 1100 Series LC/MSD (Agilent Technologies, Palo Alto, CA). YdiF protein was diluted to 0.4 mg/ml in 20% (v/v) acetonitrile, 0.1% (v/v) formic acid and ionized by direct injection. The γ-glutamyl-CoA thioester form of YdiF was prepared in a 50-μl reaction consisting of 0.15 μM YdiF, 50 mM Tris-HCl (pH 8.5), and 1 mM CoA thioester (acetyl-CoA, butyryl-CoA, propionyl-CoA, or crotonoyl-CoA) in the presence and absence of 20 mM sodium acetate. For identification of products, 2 μl of the reaction mixture following incubation at 21 °C for 2 h was injected and analysis was carried out in negative mode with the above buffer system with 10 mM ammonium acetate.

Enzyme Activity Measurements—Characterization of YdiF enzymatic activity was performed essentially according to Buckel *et al.* (20). A 1-ml reaction mixture containing 50 μM coenzyme A derivative (Sigma), 10 mM sodium acetate (or other carboxylic acid), 10 mM oxaloacetate, 10 μg of citrate synthase (Sigma), 10 mM 5,5′-dithiobis(nitrobenzoic acid), and 20 μg of purified YdiF was incubated at room temperature for 30, 60, and 120 min and the release of free coenzyme A monitored at 412 nm and detected via formation of the nitrothiobenzoate dianion. Propionate-CoA transferase from *Clostridium propionicum* (21) was used as a positive control.

Crystallization—Initial crystallization conditions were determined by hanging drop vapor diffusion using screens from Hampton Research (Laguna Hills, CA). The best YdiF crystals were obtained by equilibrating 1 μl of protein (7.5 mg/ml) in buffer (20 mM Tris-HCl, pH 8, 0.4 M NaCl, 5 mM dithiothreitol) mixed with 1 μl of reservoir solution (22.5% (w/v) polyethylene glycol 4000, 3% (v/v) isopropyl alcohol, 0.1 M Hepes, pH 7.5) and suspended over 1 ml of reservoir solution. Crystals grew to a size of ~0.1 × 0.1 × 0.06 mm in 2 days at 21 °C. For data collection, crystals were transferred for 1 min to a cryo-protectant solution containing reservoir solution supplemented with 17% (v/v) 2-methyl-2,4-pentanediol, picked up in a nylon loop, and flash cooled in a N_2 cold stream (Oxford Cryosystem, Oxford, UK). Crystals of YdiF belong to the space group $P2_1$ with unit cell dimensions $a = 80.2$, $b = 132.3$, $c = 105.1$ Å, $\beta = 100.6°$, and $Z = 8$, with a V_m of 2.4 $Å^3\ Da^{-1}$ and a solvent content of 48% (22).

Crystals of the YdiF-γ-glutamyl-CoA thioester were obtained by co-crystallization of YdiF with 10 mM acetyl-CoA, acetoacetyl-CoA, propionyl-CoA, butyryl-CoA, or crotonoyl-CoA (Sigma), and reservoir solutions containing 15.5–17.5% (w/v) polyethylene glycol 3350 and 80 mM sodium potassium tartrate. Crystals formed after 3–4 days by mixing 1 μl of 7.5 mg/ml YdiF in buffer and 1.5 μl of reservoir solution in a microbatch plate and layering it with paraffin oil. Crystals were cryoprotected by a brief transfer to a solution containing reservoir solution supplemented with 20% (v/v) glycerol and flash cooled in the nitrogen stream at 100 K. Crystals obtained in the presence of acetoacetyl-CoA, acetyl-CoA, and propionyl-CoA also belonged to space group $P2_1$ with unit cell dimensions $a = 81.1$, $b = 140.2$, $c = 112.6$ Å and $\beta = 108.2°$, whereas crystals obtained from butyryl-CoA and crotonoyl-CoA had cell dimensions $a = 80.8$, $b = 137.1$, $c = 110.4$ Å, and $\beta = 105.8°$.

Data Collection, Structure Solution, and Refinement—Diffraction data from a selenomethionine-labeled YdiF crystal were collected using a three wavelength MAD regime with a Quantum-4 CCD detector (Area Detector Systems Corp., San Diego, CA) at beamline X8C at the National Synchrotron Light Source, Brookhaven National Laboratory. Data processing and scaling was performed with HKL2000 (23) (TABLE ONE). Of 44 expected selenium atoms in the asymmetric unit, 39 were located using data to 2.7-Å resolution with the program SOLVE (24), and used to calculate phases with a resulting figure of merit of 0.55. Density modification with the program RESOLVE (25) improved the quality of the map (figure of merit = 0.73) and allowed for automated model building of 52% of main chain atoms and fitting of 26% of the expected side chains within the asymmetric unit. The partial model obtained from RESOLVE was extended manually with the help of the program O (26) and improved by several cycles of refinement using the

TABLE ONE

X-ray crystallographic data

Dataset	Selenomethionine			Apo	Glutamyl-CoA thioester[a]	Glutamyl-CoA thioester[b]
	Infl	Peak	Remote			
Unit cell						
a (Å)			79.8	81.1	80.9	81.0
b (Å)			132.4	133.3	137.1	140.2
c (Å)			105.2	105.7	112.3	112.6
β (°)			101	101	108	108
Z			8	8	8	8
Resolution (Å)	50–2.7	50–2.7	50–2.7	50–1.9	50–2.15	50–2.0
	(2.8–2.7)	(2.8–2.7)	(2.8–2.7)	(1.97–1.90)	(2.23–2.15)	(2.07–2.00)
Wavelength (Å)	0.9799	0.9795	0.9646	1.1	1.1	1.1
Observed *hkl*	278,516	173,200	249,210	491,266	427,268	561,970
Unique *hkl*	58,242	55,944	57,633	163,843	124,447	159,093
Redundancy	4.7	3.1	4.3	3.0	3.6	3.6
Completeness	98.8 (97.0)	95.0 (87.5)	98.2 (95.0)	94.3 (71.8)	98.9 (95.4)	98.8 (90.5)
R_{sym} (%)[c]	0.110 (0.437)	0.082 (0.333)	0.101 (0.391)	0.053 (0.284)	0.063 (0.483)	0.079 (0.454)
I/σ (I)	8.4 (2.2)	10.2 (2.6)	9.6 (2.6)	20.1 (4.4)	11.9 (2.1)	9.0 (2.0)
Wilson B $(Å)^2$				25.2	34.6	25.8
Refinement statistics						
Resolution (Å)				50–1.9	50–2.15	50–2.00
R_{work} (No. *hkl*)[d]				0.187 (148,789)	0.186 (112,953)	0.184 (142,009)
R_{free} (No. *hkl*)				0.221 (15,015)	0.235 (11,494)	0.224 (14,361)
B-factor $(Å)^2$/No. atoms						
Protein				27.0 (15,700)	35.3 (15,364)	25.0 (15,604)
Solvent				39.0 (1,271)	41.1 (1,304)	34.3 (1,478)
Ligands					56.4 (168)	49.9 (208)
Ramachandran						
Allowed (%)				99.1	99.3	99.4
Generous (%)				0.8	0.5	0.5
Disallowed (%)				0.1	0.2	0.2
r.m.s. deviations						
Bonds (Å)				0.009	0.010	0.009
Angles (°)				1.259	1.250	1.200
PDB code				2AHU	2AHW	2AHV

[a] Glutamyl-CoA thioester intermediate derived from butyryl-CoA.
[b] Glutamyl-CoA thioester intermediate derived from acetyl-CoA.
[c] $R_{sym} = (\Sigma|I_{obs} - I_{avg}|)/\Sigma I_{avg}$.
[d] $R_{work} = (\Sigma|F_{obs} - F_{calc}|)/\Sigma F_{obs}$.

TABLE TWO

***In vitro* activity of YdiF**

Substrate	Co-substrate	Specific activity
		μmol/min/mg
Acetoacetyl-CoA	Acetate	11.5
Propionyl-CoA	Acetate	9.6
Crotonoyl-CoA	Acetate	7.3
Butyryl-CoA	Acetate	6.3
Propionyl-CoA	Succinate	ND[a]
Acetyl-CoA	Acetoacetate	–[b]
Acetyl-CoA	Propionate	3.6
Acetyl-CoA	Butyrate	4.5
Acetyl-CoA	Isobutyrate	3.2
Acetyl-CoA	4-OH-butyrate	0.9
Acetyl-CoA	Isovalerate	ND

[a] ND, no reaction detected by mass spectrometry.
[b] Specific activity could not be determined due to unstable product.

program REFMAC (27). Neither non-crystallographic symmetry restraints nor a σ-cutoff were used during refinement.

The histidine tag and residues 1–3, 277–283, and 343–348 were disordered in the electron density map. The final model of apo-YdiF includes four independent monomers, each consisting of residues 4–276, 284–342, and 349–529 with good stereochemistry (PROCHECK, Ref. 28). The model also includes 1271 water molecules and has an *R*-factor of 0.187 and R_{free} of 0.221 for all data to 1.9-Å resolution (TABLE ONE).

Diffraction data for YdiF co-crystallized with various CoA thioesters were collected at beamline X29, National Synchrotron Light Source, using a Quantum-315 CCD detector (ADSC). Datasets were obtained as follows: acetoacetyl-CoA (2.4 Å), acetyl-CoA (2.0 Å), propionyl-CoA (2.1 Å), butyryl-CoA (2.15 Å), and crotonoyl-CoA (2.4 Å). The structures of YdiF-CoA complexes were determined by molecular replacement using the program MOLREP (29) with the apo-YdiF tetramer as the search model. Comparison of electron density maps for each of the datasets collected showed very similar features in the active site region, therefore, only data from acetyl-CoA and butyryl-CoA co-crystals, which showed good density for CoA, were used to build and refine models of the CoA complex. In subunit D of the YdiF-CoA complex obtained from the butyryl-CoA co-crystals the C-terminal domain is less well ordered because of few crystal lattice contacts. These models were refined using REFMAC to a final *R*-value of 0.184 (R_{free} of 0.224) for the CoA thioester complex derived from acetyl-CoA, and an *R*-value of 0.186 (R_{free} of 0.235) for the same complex derived from butyryl-CoA, respectively. Final refinement statistics are shown in TABLE ONE.

RESULTS AND DISCUSSION

YdiF Is an Acyl-CoA Transferase

YdiF is grouped with ~330 other proteins in the coenzyme A transferase superfamily IPR004165 (InterPro data base (30)) with rather diverse substrate specificities (31–35). Within the *E. coli* K12 genome, the individual N-terminal domain (residues 12–255) and C-terminal domain (residues 285–512) of YdiF are related in sequence to AtoD (24% identity) and AtoA (25% identity), representing the α- and β-subunits, respectively, of ACT (36). The highest similarity to a CoA transferase with an experimentally verified function is for propionyl-CoA transferase from *C. propionicum*, which shows 45% sequence identity with YdiF (21), leading to the possibility that YdiF possesses this function. YdiF also shows 23% sequence identity to SCOT from pig heart (37). The N- and C-terminal domains of YdiF show 16 and 18% identity, respectively, with the α- and β-subunits of GCT (38).

As CoA transferases can exhibit a broad activity profile toward different CoA donors and acceptors (20, 39, 40), various acyl-CoA thioesters were tested for *in vitro* activity with YdiF. Among the CoA derivatives tested, acetoacetyl-CoA exhibited the highest activity with acetate as an acceptor. When acetyl-CoA was used as the donor, YdiF utilized propionate, acetoacetate, butyrate, isobutyrate, and 4-hydroxybutyrate as acceptors but not isovalerate (TABLE TWO). No free CoA could be detected when the enzyme was incubated with CoA derivatives in the absence or presence of co-substrate. Overall, the activity profile of YdiF with various CoA thioesters resembles that of ACT (39). Based on the activity profile and sequence analysis, we speculate that YdiF plays a role in short-chain fatty acid metabolism in *E. coli* (41, 42).

Monomer Structure

The asymmetric unit contains four nearly identical YdiF monomers, with any pair of them superimposing with a root mean square deviation between 0.26 and 0.41 Å for all Cα atoms. Each YdiF monomer consists of two domains, an N-terminal domain (Val^4-Pro^{254}) and C-terminal domain (Leu^{285}-Ala^{529}), each having an open α/β-protein fold. A polypeptide linker (Asp^{255}-Pro^{284}) connects these two domains. The N-terminal domain is made of three layers, with the core being a central, eight-stranded parallel β-sheet with one anti-parallel edge strand. On one side of this sheet, near its center, are two α-helices flanked on either side by a 4-stranded and 3-stranded mixed β-sheet, respectively, together forming a second layer. The third layer, on the opposite side of the central β-sheet, is made of three α-helices and a short helical turn (Fig. 1*a*). The C-terminal domain has a very similar three-layered architecture with a central, 10-stranded mixed β-sheet with three α-helices and a β-hairpin on one side forming the domain interface, and two α-helices and a helical turn on the other, solvent-exposed side. The two domains associate to form a bowl-like shape with a deep cleft between them, and the active site located at the bottom of the bowl. Residues forming the domain interface are located in regions 94–150, 203–210, and 265–273 of the N-terminal domain and 334–347, 390–407, and 449–460 of the C-terminal domain.

The three-dimensional structure clearly indicates an ancestral gene duplication event. The N- and C-terminal domains can be superimposed with a r.m.s. deviation of 1.6 Å for 85 Cα pairs. Structure-based sequence alignment of these two domains shows several long insertions

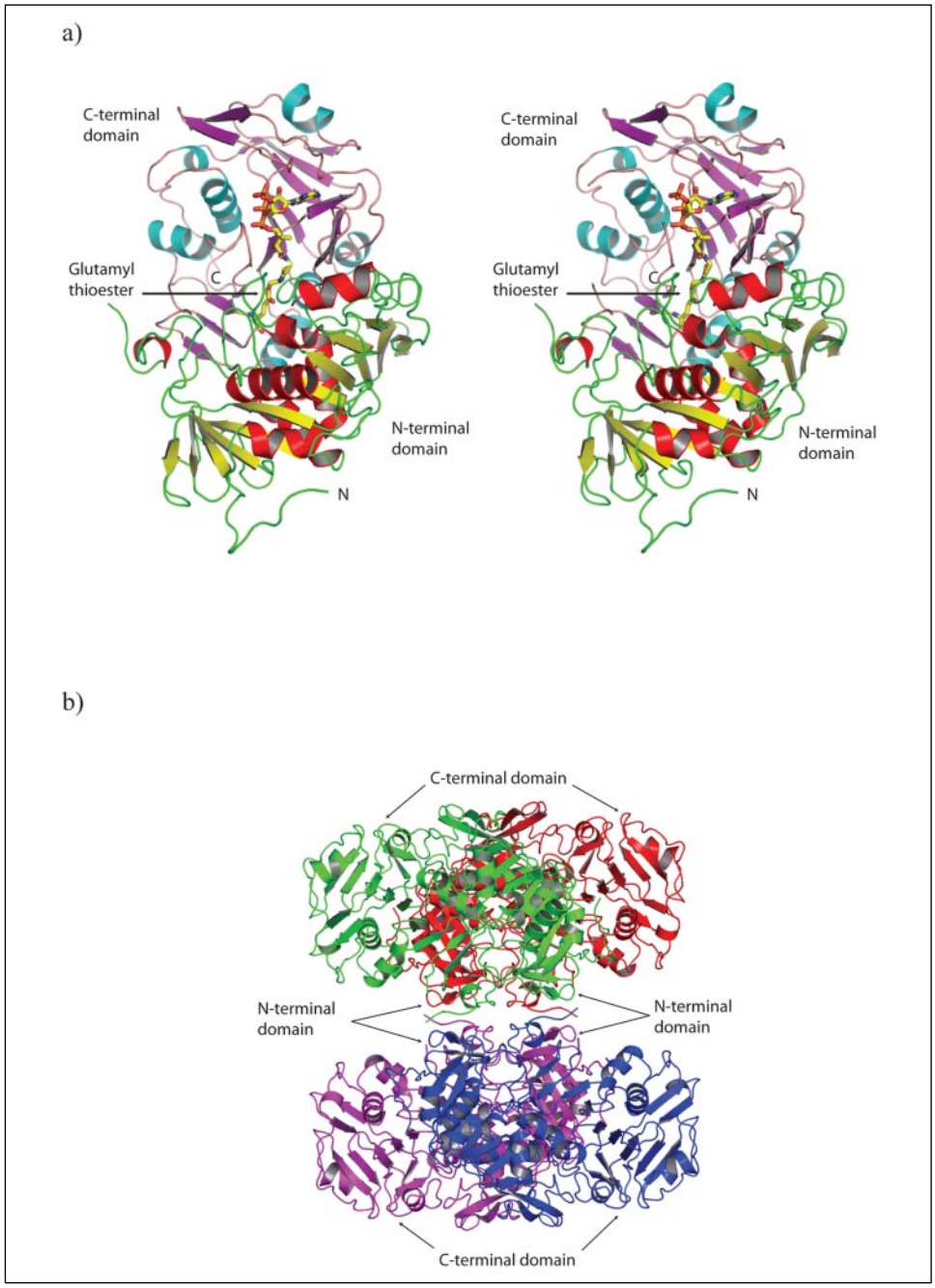

FIGURE 1. *a*, stereo view of the YdiF monomer, with secondary structure elements colored *yellow* and *red* (N-terminal domain) or *cyan* and *magenta* (C-terminal domain). The glutamyl-CoA thioester is depicted in *stick* representation. *b*, the YdiF tetramer, with the two dimers that form the tetramer colored either *green* and *red*, or *purple* and *blue*, respectively. This figure was prepared with the program Pymol.

in different locations (result not shown). The very low level of sequence identity retained between the two domains (~6%) suggests that this gene duplication event occurred in the distant past. A similar ancient gene duplication event has been postulated for the α- and β-subunits of GCT, which together form the active heterodimer (14).

Quaternary Structure

YdiF forms tetramers in solution, as determined by both gel filtration and dynamic light scattering studies. The crystal structure shows that the YdiF tetramer is formed as a dimer of dimers having pseudo 222 symmetry, with the two dimers (AB or CD) associating tightly along the pseudo 2-fold axis (Fig. 1*b*). The contacts between dimers are less pronounced than those involved in dimer formation, with a buried area of ~1470 Å^2 or ~4% per dimer. At the dimer-dimer interface, the N-terminal domain of each monomer (A or B, respectively) makes contacts (<4 Å) with only one monomer (C or D, respectively) of the second dimer. The dimer-dimer interface of the tetramer contains more ordered water molecules resulting in additional bridging hydrogen bonds than the monomer-monomer interface of the dimer. The associations of the monomers into a tetramer are such that the substrate binding clefts of each monomer remain solvent exposed.

Intermolecular contacts of the dimer involve both the N- and C-terminal domains of the protein and are predominantly van der Waals interactions with few hydrogen bonds. An intramolecular salt bridge between Arg^{126} of the N-terminal domain and Asp^{364} in the C-terminal domain at the center of the dimer interface contributes to stabilization. The surface area buried as a result of dimerization is ~2,600 Å^2 per monomer, corresponding to 12% of the total monomer surface area. The two independent dimers can be superimposed with a r.m.s. deviation of 0.28 Å, identical to that for individual monomers, indicating a

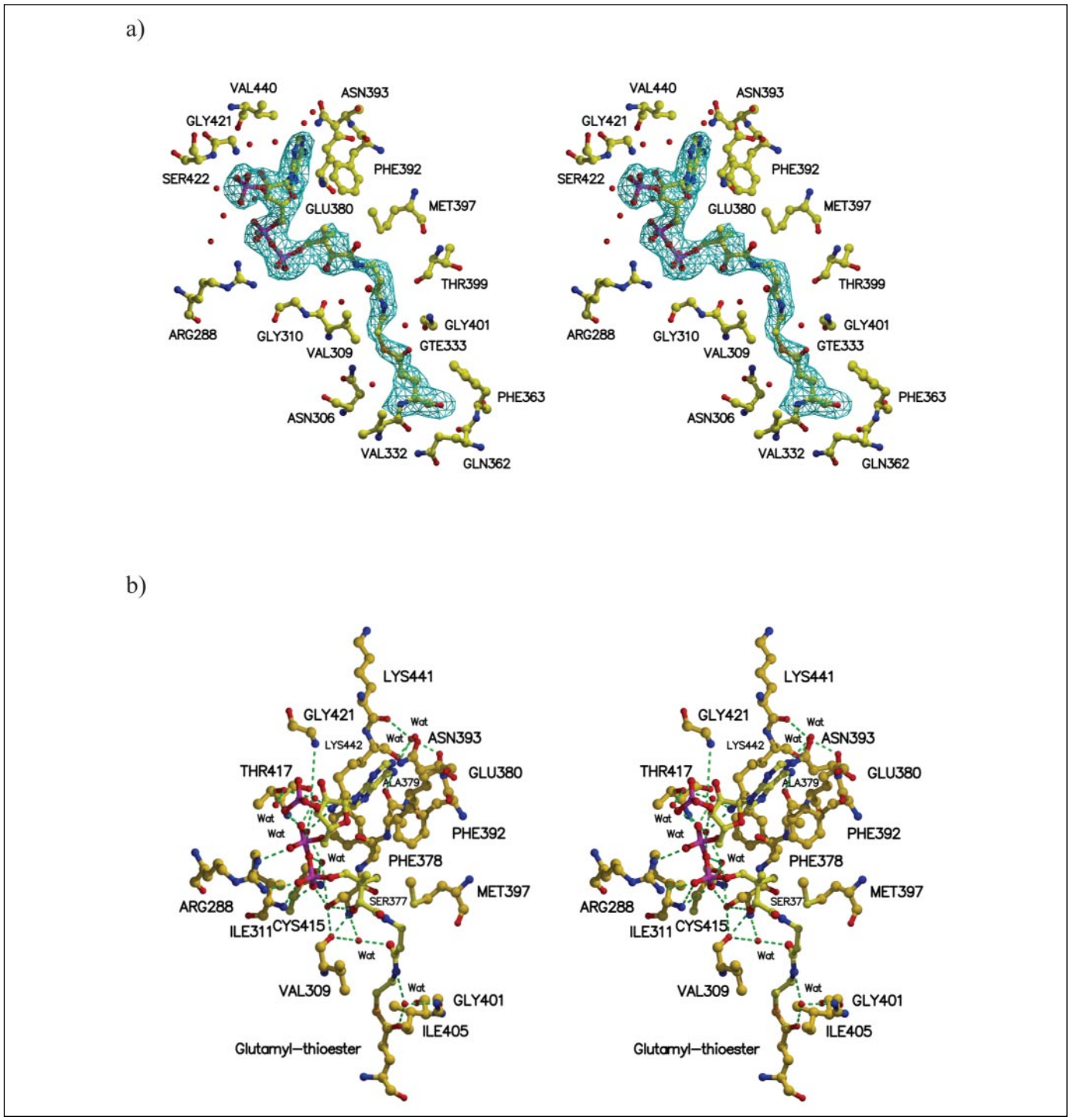

FIGURE 2. *a*, stereo $F_o - F_c$ (omit) electron density contoured at 2.5σ for the γ-glutamyl-CoA thioester bound to Glu^{333} resulting from co-crystallization with butyryl-CoA, with the final model superimposed. The CoA ligand and Glu^{333} were omitted prior to refinement. *b*, stereo view of the binding site of the CoA thioester intermediate, with hydrogen bonds shown with *dashed lines*. The thioester intermediate is colored by a CPK scheme.

rigid association of monomers into the dimer. Of 65 residues involved in YdiF dimer formation, Arg^{126}, Pro^{133}, Gly^{134}, Asp^{192}, Val^{240}, Pro^{243}, and Leu^{246} are conserved in SCOT and other YdiF-related sequences, whereas no residues involved in tetramer formation are conserved.

Complex with Coenzyme A

To define the substrate binding site and residues involved in catalysis we co-crystallized YdiF with several coenzyme A thioesters in the absence of the acceptor co-substrate, resulting in trapping of CoA in the form of its γ-glutamyl-CoA thioester. The extent of electron density observed for CoA varied in the different subunits obtained from the various data sets. In the crystal structure of YdiF co-crystallized with butyryl-CoA, electron density corresponding to that of a covalent thioester between Glu^{333} and CoA was observed in subunits A, B, and C (Fig. 2*a*). In these three subunits, the phosphoadenosine moiety showed stronger electron density compared with that for the pantetheine moiety. In subunit D, the electron density was weaker for both the phosphoadenosine as well as the pantetheine moieties, and density consist-

ent with a covalent thioester was not observed. In YdiF co-crystallized with acetyl-CoA, electron density for the thioester linkage could be observed in the A and C subunits. Good density for the phosphoadenosine moiety and weak density for pantetheine portion of CoA, with no continuous density to Glu^{333}, was observed in subunits B and D. In subunit B, the Glu^{333} side chain was weakly defined, suggesting it assumes several conformations.

CoA binds in the cleft formed at the interface of the N- and C-terminal domains, with all interactions with CoA coming from the C-terminal domain (Fig. 2*b*). The interactions between YdiF and CoA are the same in all subunits. The CoA binding pocket is formed by residues 306–311, an extended "flap" (389–402) and residues 419–423 and 440–442. Binding of CoA results in localized structural changes for residues 300–315 and 410–430 and the side chains of Arg^{288} and Phe^{392}. Superposing the tetramers of apo-YdiF and the CoA thioester complex gives a r.m.s. deviation of 0.6 Å for all main chain atoms indicating that CoA binding causes no large structural changes.

The portion of CoA making the most abundant protein interactions is the diphosphate moiety, which is hydrogen-bonded to the side chains of Arg^{288} and Ser^{377}, to the main chain amide of Ile^{311} and through bridging waters to the NH groups of Phe^{378} and Thr^{417}, the carbonyl of Cys^{415}, and the side chains of Lys^{442} and Thr^{417} (Fig. 2*b*). The O-2′ atom of ribose is hydrogen bonded to the NH group of Gly^{421}. Finally, the adenine N-6 atom forms hydrogen bonds to the backbone carbonyl of Ala^{379} and through a bridging water molecule to the side chain of Glu^{380} and the carbonyl of Lys^{441}, whereas the N-1 ring atom contacts Glu^{380} and Asn^{393} through water molecules. The adenine ring also makes a herringbone contact with the ring of Phe^{392}. The pantetheine moiety predominantly makes van der Waals contacts within the mainly hydrophobic bottom part of the binding pocket (residues 309–310, 376–379, and 389–405). A water-mediated hydrogen bond is observed between the pantetheine N-4 atom and the NH of Gly^{401}, whereas a second water bridges the pantetheine O-5 atom with the carbonyl of Val^{309} and NH of Ser^{377}. Concomitant with CoA binding, the electron density for the side chains of Val^{309}, Met^{397}, and Ile^{405} becomes somewhat more diffuse, consistent with mobility of the pantetheine portion of CoA.

Formation of the γ-glutamyl-CoA thioester in solution was verified by electron spray ionization-mass spectrometry following incubation of YdiF with butyryl-CoA, revealing a single species corresponding to a mass of 60,379 Da, which is 751 Da in excess of the native molecular mass of 59,628 Da, with no mass corresponding to the apoprotein being observed. The excess mass corresponds well to the expected mass difference of 749 Da for the covalent γ-glutamyl-CoA thioester formed between the thiol group of CoA and the carboxyl of Glu^{333}, as supported by the crystallographic evidence herein. Detection of only the γ-glutamyl-CoA thioester confirms that in the absence of co-substrate, the reaction stops at this intermediate, as previously observed by MS with GCT (10) and SCOT (43), or by enzymatic assay with SCOT (44, 45).

Catalytic Site

In all YdiF-related CoA transferases, the sequence motifs $^{333}EXGXXG^{338}$ and $^{398}GXGG(A/F)^{402}$ are conserved, with the former sequence containing the catalytic glutamate residue (10, 46, 47) and the latter forming the oxyanion hole (14). In those subunits that show electron density for CoA, Glu^{333} adopts one of two extended orientations. Where the density is consistent with formation of the γ-glutamyl-CoA thioester, Glu^{333} (conformation I) forms a water-mediated hydrogen bond to the amide of Gly^{401} (Fig. 3*a*). In this conformation, Asn^{306} is re-positioned so that it forms a hydrogen bond with the main chain atoms of Tyr^{375} and CO of Val^{307}. In subunit D of the complex obtained using acetyl-CoA, Glu^{333} is not involved in a covalent interaction with CoA (conformation II) but forms a hydrogen bond with Gln^{118}, and through a water molecule to the amide of Gly^{401} (Fig. 3*b*). In the native structure, Glu^{333} assumes a bent conformation (conformation III) in all four subunits, and is stabilized by side chain hydrogen bonds to Asn^{306} and, through a bridging water molecule to Gln^{118} and NH of Gly^{401} (Fig. 3*c*). Binding of CoA, and the concomitant change in orientation of Glu^{333}, results in breakage of its hydrogen bond with Asn^{306}. Together, these results show that the catalytic Glu^{333} in YdiF adopts three distinct conformations during the catalytic cycle.

Comparisons with Family I CoA Transferases

Overall Fold—The structures of the individual YdiF domains closely resemble those of SCOT (16), the α- and β-subunits of the GCT heterodimer (14), and the ACT α-subunit (15), with a r.m.s. deviation of 1.4–1.6 Å for the Cα atoms in pairwise structural alignments. When full-length YdiF and SCOT monomers are superimposed, the r.m.s. deviation is greater, because of a small difference in the relative orientation of the domains connected by a flexible linker. These domains are grouped into the NagB/RpiA/CoA transferase fold in SCOP (48) sharing a common α/β/α architecture and a central 6-stranded β-sheet. The α- and β-subunits are classified into individual superfamilies within this fold.

Close examination of YdiF, SCOT, and GCT shows subtle but significant differences between them. In YdiF, the 341–347 loop located near the putative active site is ~10 residues shorter than in SCOT and β-GCT. A second insertion between residues 129–130 of α-ACT is present in YdiF-(147–163), SCOT-(128–147), and α-GCT-(131–152). In addition, YdiF has an N-terminal extension (Val^{4}-Arg^{12}) and a long insertion encompassing residues 420–439 that is found in neither SCOT nor GCT.

CoA Binding Site—Comparing the CoA binding region of YdiF with SCOT (C-terminal domain, Protein Data Bank code 1OOY) and β-GCT (subunit, PDB 1POI) reveals that spatially similar elements of secondary structure interact with CoA. Structurally similar residues involved with CoA binding, in addition to the catalytic glutamate residue, Glu^{333} (Glu^{305} of SCOT or Glu^{54} of β-GCT), include Arg^{288}, Val^{307}, Gly^{308}, Gly^{310}, Leu^{376}, Ala^{379}, Phe^{392}, Gly^{400}, Gly401, Ile^{405}, and Lys^{442} (Fig. 3*d*). Several of these residues are in the vicinity of the pantetheine moiety. Based on these observations, both SCOT and GCT would be expected to exhibit similar binding interactions with CoA as does YdiF. However, the structural superposition indicates that SCOT would require an inter-domain movement to effectively interact with CoA, as has been suggested earlier (11).

Co-substrate Binding Site—Little experimental data are available about specific residues of Family I CoA transferases that are involved in co-substrate binding. Comparison of the active site regions of YdiF, SCOT, and GCT suggests that the residues likely to be involved in co-substrate binding differ among these enzymes. In YdiF, these include the structurally conserved residue Gln^{118}, and the non-conserved residues Gly^{37}, Thr^{69}, Gly^{70}, His^{95}, and Gln^{99}. Additional residues proposed to participate in co-substrate binding in GCT (14) are part of the insertion region (76–84) and are absent in YdiF. The shorter 341–347 loop in YdiF results in the cleft being more open and accessible to the co-substrate, whereas in contrast, the longer loops in SCOT and β-GCT results in narrowing of the cleft.

Mechanism of Action—In Family I CoA transferases, the catalytic transfer of coenzyme A from the acyl-CoA thioester to the carboxylic acid co-substrate occurs by two half-reactions in a ping-pong kinetic mechanism (40, 49) with the formation of a covalent thioester interme-

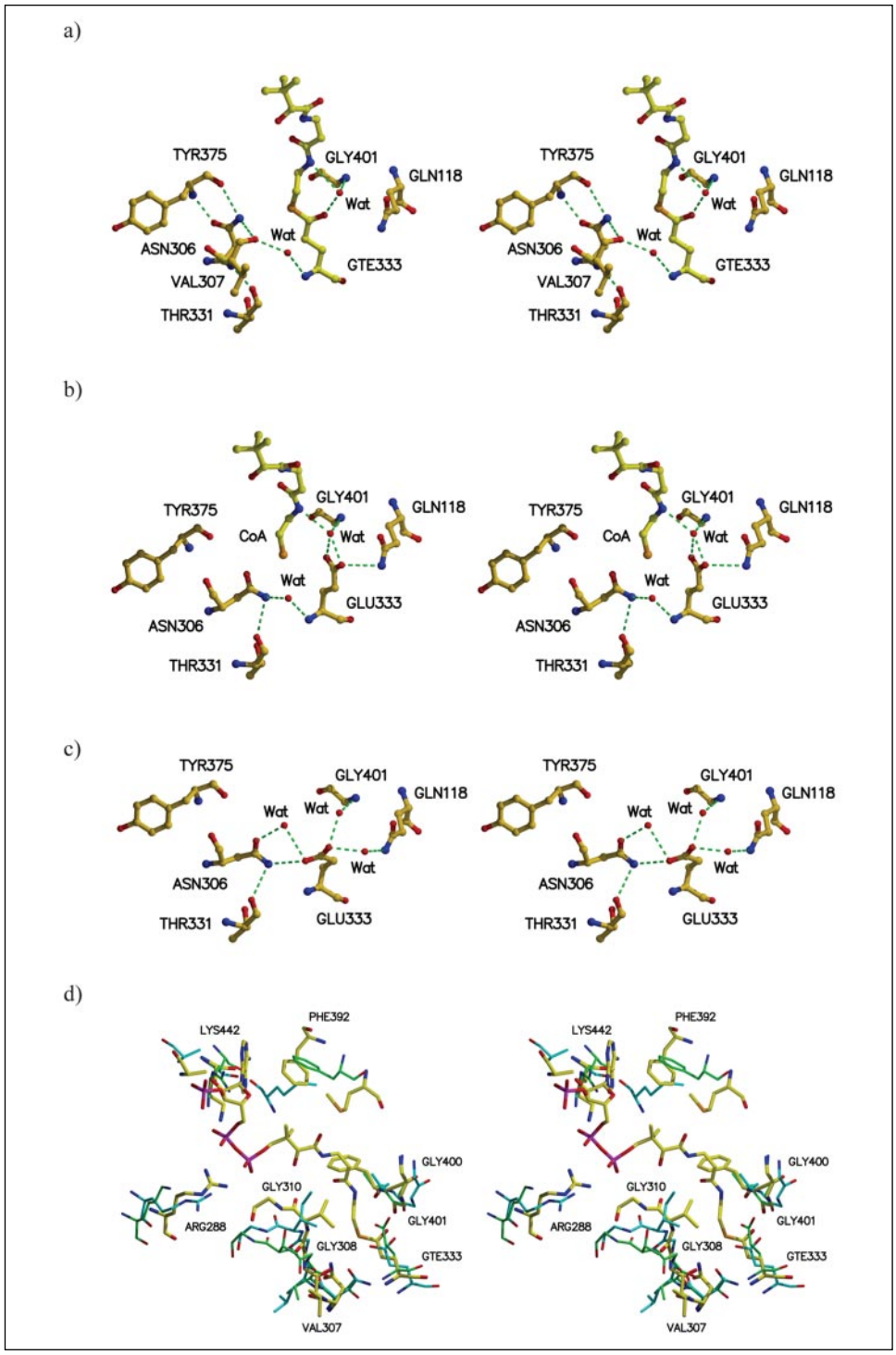

FIGURE 3. **Changes in orientation and hydrogen bonding interactions of Glu^{333} in the YdiF active site and comparison of CoA binding sites.** *a*, the γ-glutamyl-CoA thioester intermediate (*GTE*) (conformation I); *b*, alternate conformation from subunit D (conformation II); and *c*, apo-YdiF (conformation III). *d*, superposition of the C-terminal domains of YdiF (*yellow*) and SCOT (*cyan*) and the β-subunit of GCT (*green*), with structurally conserved residues corresponding to YdiF labeled. *GTE* designates the γ-glutamyl-CoA thioester intermediate.

diate between coenzyme A and the active site glutamate residue (7). The reaction mechanism has previously been investigated in detail, and determined to consist of several steps (Fig. 4). In the first step, the glutamate side chain attacks the carbonyl carbon of the thioester linkage, resulting in breakage of the CoA thioester bond and formation of a glutamyl anhydride intermediate (*A*). In the second step, the sulfur anion of CoA attacks the carbonyl carbon of the catalytic glutamate resulting in a covalent γ-glutamyl-thioester intermediate (*B*) and concomitant release of the donor carboxylic acid. In the third step, the carboxyl oxygen of the acceptor carboxylic acid co-substrate attacks the carbonyl carbon of the glutamate side chain, liberating CoA from the glutamyl-thioester intermediate and generating a second anhydride intermediate (*C*). In the final step, the sulfur anion of CoA attacks the carbonyl carbon of the acceptor carboxylic acid and forms an acyl-CoA, leaving glutamate in its starting state.

From the crystal structure of the YdiF-CoA complex it is seen that three residues, Gln^{118}, Asn^{306}, and Glu^{333} play a crucial role in the CoA transferase reaction. The principle role of Gln^{118} is proposed to be in the stabilization of the catalytic glutamate residue in a conformation suitable for formation of the anhydride intermediate with the carboxylic acid.

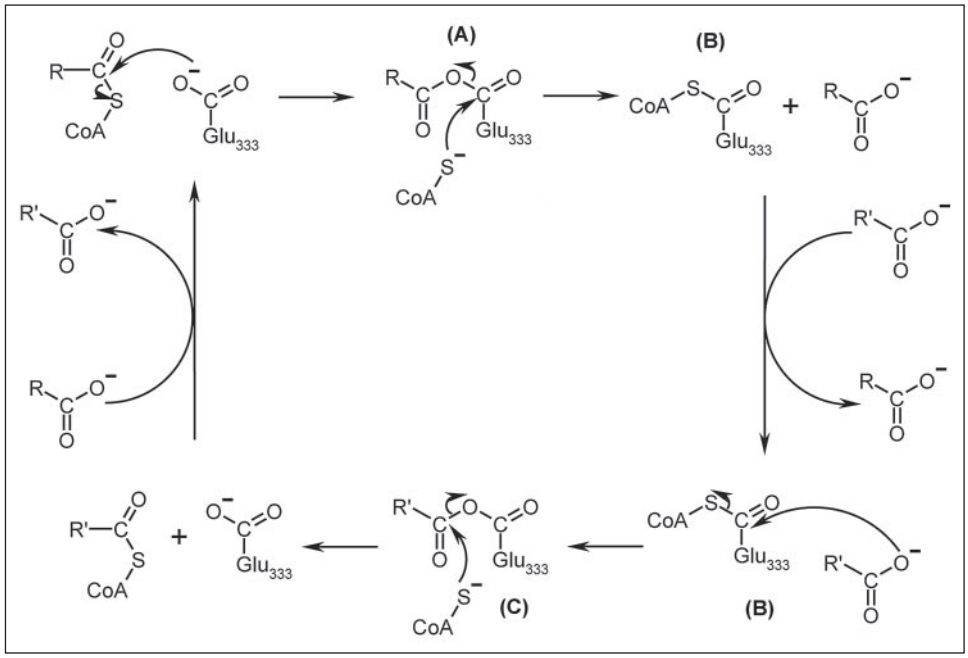

FIGURE 4. **Chemical mechanism previously proposed for SCOT and common to other Family I CoA transferases (16).** The two anhydride intermediates (*A* and *C*) as well as the covalent CoA thioester intermediate (*B*) are depicted.

The glutamine residues equivalent to Gln^{118} of YdiF in α-GCT and in SCOT show similar interactions with the catalytic glutamate. In the structures of YdiF complexes, the side chain of Glu^{333} is observed in two conformations: one in which it forms a thioester intermediate with CoA (conformation I) and another in which it would aid in formation of the anhydride intermediate (conformation II). In this second conformation, the side chain of Glu^{333} points toward the predicted co-substrate binding site, where it would need to form an anhydride during the catalytic cycle. The two conformations of Glu^{333} differ from that found in the native structure (Fig. 3). Whereas only a single conformation of Glu^{333} is found in apo-YdiF, the corresponding catalytic Glu^{305} in apo-SCOT displays different conformations in different subunits, which correspond well to the three conformations in the various YdiF structures. Asn^{306} is involved in stabilizing Glu^{333} in its resting position when no acyl-CoA is bound. However, during the formation of the γ-glutamyl-thioester intermediate Asn^{306} assumes a different orientation. The movement of Glu^{333} from conformation I to II as a covalent thioester results in re-positioning of Asn^{306} and in the changes in hydrogen bonding interactions that we observe (Fig. 3). Because of the absence of bound CoA in SCOT, only one orientation of Asn^{281}, equivalent to Asn^{306} of YdiF, is observed, regardless of the conformation of the catalytic Glu^{305} (PDB 1M3E, Ref. 16).

Based on these findings, the structural basis for the mechanism of action of Family I CoA transferases is proposed. Upon binding of the acyl-CoA, Glu^{333} re-orients from its resting position (conformation III) to adopt an extended conformation (II) with a concomitant shift in the main chain atoms of the 332–334 loop. This would favor attack on the carbonyl carbon of the thioester leading to formation of an anhydride intermediate between Glu^{333} and carboxylic acid. As previously proposed (14), the oxyanion hole in YdiF would serve to neutralize the developing negative charge in the transition state. The anhydride intermediate would be stabilized by a hydrogen bond to Gln^{118}. Attack of the sulfur anion at the side chain carbonyl carbon of Glu^{333} results in formation of the covalent thioester intermediate, repositioning of Glu^{333} from conformation II to I, as well as movement of the 306–312 loop and of the pantetheine moiety of CoA (Fig. 3). Binding of the co-substrate initiates the second half-reaction, and movement of Glu^{333} from conformation I to II. The remaining steps are essentially an inverse of the first half-reaction.

Biochemical evidence for the formation of an enzyme-bound covalent γ-glutamyl-CoA thioester intermediate for Family I CoA transferases has been provided previously (7, 44). Here, we complement and extend previous studies by employing x-ray crystallography to view the molecular details of the γ-glutamyl-CoA thioester intermediate. It has been shown that the pantetheine portion of CoA destabilizes the E-CoA covalent intermediate, but stabilizes the transition state, together resulting in an acceleration of the second half-reaction in SCOT (12, 13). In contrast, binding of the nucleotide portion of CoA has been shown to be strongly stabilizing in both the E-CoA intermediate and transition states, and weak in the Michaelis complex. The function of the nucleotide portion of CoA has been described as to "pull " the pantetheine moiety into the active site where it becomes highly reactive (12). Structural evidence consistent with these results is provided by the present structure where we observe that the electron density for the nucleotide portion of CoA is always stronger, and therefore better ordered, than that of the pantetheine moiety. In the YdiF-CoA complex, the polar atoms of the pantetheine moiety are surrounded mainly by a hydrophobic environment, which may account for at least part of the destabilizing effect of this group in the E-CoA intermediate.

Conclusions

In this study we have trapped the CoA thioester intermediate of YdiF, and compared the CoA binding site to those of other Family I CoA transferases. Clear similarities in the modes of CoA recognition by all these enzymes are evident, although there are structural differences in their co-substrate binding sites. It is clear from this study that the catalytic glutamate changes its conformation along the reaction pathway that differs between the unbound state, anhydride, and thioester intermediate, and helps to rationalize the previously observed multiple conformations of the catalytic glutamate in the structures of SCOT and GCT. The previously suggested mobility of the pantatheine moiety of CoA, supported by our crystallographic studies, plays an important role in catalysis and is expected to be observed in other members of Family I CoA transferases.

Acknowledgments—We thank M. McMillan, L. Flaks, and H. Robinson for assistance in synchrotron x-ray data collection, and T. Selmer for providing C. propionicum propionate-CoA transferase. Data for this study were measured at beamlines X8C, X26C, and X29 of the National Synchrotron Light Source. Financial support comes principally from the Office of Biological and Environmental Research and of Basic Energy Sciences of the United States Department of Energy, and the National Center for Research Resources of the National Institutes of Health.

REFERENCES

1. Mishra, P. K., and Drueckhammer, D. G. (2000) *Chem. Rev.* **100,** 3283–3309
2. Knudsen, J., Jensen, M. V., Hansen, J. K., Faergeman, N. J., Neergaard, T. B., and Gaigg, B. (1999) *Mol. Cell Biochem.* **192,** 95–103
3. Engel, C., and Wierenga, R. (1996) *Curr. Opin. Struct. Biol.* **6,** 790–797
4. Fukao, T., Mitchell, G. A., Song, X-Q., Nakamura, H., Kassovska-Bratinova, S., Orii, K. E., Wraith, J. E., Besley, G., Wanders, R. J. A., Niezen-Koning, K. E., Berry, G. T., Palmieri, M., and Kondo, N. (2000) *Genomics* **68,** 144–151
5. Berry, G. T., Fukao, T., Mitchell, G. A., Mazur, A., Ciafre, M., Gibson, J., Kondo, N., and Palmier, M. J. (2001) *J. Inherit. Metab. Dis.* **24,** 587–595
6. Heider, J. (2001) *FEBS Lett.* **509,** 345–349
7. Solomon, F., and Jencks, W. P. (1969) *J. Biol. Chem.* **244,** 1079–1081
8. Jonsson, S., Ricagno, S., Lindqvist, Y., and Richards, N. G. J. (2004) *J. Biol. Chem.* **279,** 36003–36012
9. Ricagno, S., Jonsson, S., Richards, N., and Lindqvist, Y. (2003) *EMBO J.* **22,** 3210–3219
10. Selmer, T., and Buckel, W. (1999) *J. Biol. Chem.* **274,** 20772–20778
11. White, H., Solomon, F., and Jencks, W. P. (1976) *J. Biol. Chem.* **251,** 1700–1707
12. Fierke, C. A., and Jencks, W. P. (1986) *J. Biol. Chem.* **261,** 7603–7606
13. Whitty, A., Fierke, C. A., and Jencks, W. P. (1995) *Biochemistry* **34,** 11678–11689
14. Jacob, U., Mack, M., Clausen, T., Huber, R., Buckel, W., and Messerschmidt, A. (1997) *Structure* **5,** 415–426
15. Korolev, S., Koroleva, O., Petterson, K., Gu, M., Collart, F., Dementieva, I., and Joachimiak, A. (2002) *Acta Crystallogr. Sect. D Biol. Sci.* **58**, 2116–2121
16. Bateman, K. S., Brownie, E. R., Wolodko, W. T., and Fraser, M. E. (2002) *Biochemistry* **41,** 14455–14462
17. Coros, A. M., Swenson, L., Wolodko, W. T., and Fraser, M. E. (2004) *Acta Crystallogr. Sect. D Biol. Sci.* **60**, 1717–1725
18. Perna, N. T., Plunkett, G. I., Blattner, F. R., Mau, B., and Blattner, F. R. (2001) *Nature* **409,** 529–533
19. Hendrickson, W. A., Horton, J. R., and LeMaster, D. M. (1990) *EMBO J.* **9,** 1665–1672
20. Buckel, W., Dorn, U., and Semmler, R. (1981) *Eur. J. Biochem.* **118,** 315–321
21. Selmer, T., Willianzheimer, A., and Hertzel, M. (2002) *Eur. J. Biochem.* **269,** 372–380
22. Matthews, B. W. (1968) *J. Mol. Biol.* **33,** 491–497
23. Otwinowski, Z., and Minor, W. (1997) *Methods Enzymol.* **276,** 307–326
24. Terwilliger, T. C., and Berendzen, J. (1999) *Acta Crystallogr. Sect. D Biol. Sci.* **55**, 849–861
25. Terwilliger, T. C. (2003) *Acta Crystallogr. Sect. D Biol. Sci.* **59**, 38–44
26. Jones, T. A., Zhou, J. Y., Cowan, S. W., and Kjeldgaard, M. (1991) *Acta Crystallogr. Sect. A* **47**, 110–119
27. Murshudov, G. N., Vagin, A. A., and Dodson, E. J. (1997) *Acta Crystallogr. Sect. D Biol. Sci.* **53**, 240–255
28. Laskowski, R. A., MacArthur, M. W., Moss, D. S., and Thornton, J. M. (1993) *J. Appl. Crystallogr.* **26,** 283–291
29. Vagin, A. A., and Isupov, M. N. (2001) *Acta Crystallogr. Sect. D Biol. Sci.* **57**, 1451–1456
30. Apweiler, R., Attwood, T. K., Bairoch, A., Bateman, A., Birney, E., Biswas, M., Bucher, P., Cerutti, L., Corpet, F., Croning, M. D., Durbin, R., Falquet, L., Fleischmann, W., Gouzy, J., Hermjakob, H., Hulo, N., Jonassen, I., Kahn, D., Kanapin, A., Karavidopoulou, Y., Lopez, R., Marx, B., Mulder, N. J., Oinn, T. M., Pagni, M., Servant, F., Sigrist, C. J., and Zdobnov, E. M. (2001) *Nucleic Acids Res.* **29,** 37–40
31. Göbel, M., Kassel-Cati, K., Schmidt, E., and Reineke, W. (2002) *J. Bacteriol.* **184,** 216–223
32. Parales, R. E., and Harwood, C. S. (1992) *J. Bacteriol.* **174,** 4657–4666
33. Cary, J. W., Petersen, D. J., Papoutsakis, E. T., and Bennett, G. N. (1990) *Appl. Environ. Microbiol.* **56,** 1576–1583
34. Corthésy-Theulaz, I. E., Bergonzelli, G. E., Henry, H., Bachmann, D., Schorderet, D. F., Blum, A. L., and Ornston, L. N. (1997) *J. Biol. Chem.* **272,** 25659–25667
35. Steinmann, D., Koplin, R., Puhler, A., and Niehaus, K. (1997) *Arch. Microbiol.* **168,** 441–447
36. Jenkins, L. S., and Nunn, W. D. (1987) *J. Bacteriol.* **169,** 42–52
37. Lin, T. W., and Bridger, W. A. (1992) *J. Biol. Chem.* **267,** 975–978
38. Mack, M., Bendrat, K., Zelder, O., Eckel, E., Linder, D., and Buckel, W. (1994) *Eur. J. Biochem.* **226,** 41–51
39. Sramek, S. J., and Frerman, F. E. (1975) *Arch. Biochem. Biophys.* **171,** 14–26
40. White, H., and Jencks, W. P. (1976) *J. Biol. Chem.* **6,** 1688–1699
41. Nunn, W. D. (1986) *Microbiol. Rev.* **2,** 179–192
42. Nunn, W. D. (1996) in *Escherichia coli* and *Salmonella typhimurium*, pp. 285–301, Second Edition, ASM Press, Washington. D. C.
43. Lloyd, A. J., and Shoolingin-Jordan, P. M. (2001) *Biochemistry* **40,** 2455–2467
44. Hersh, L. B., and Jencks, W. P. (1967) *J. Biol. Chem.* **242,** 339–340
45. Hersch, L. B., and Jencks, W. P. (1967) *J. Biol. Chem.* **242,** 3481–3486
46. Mack, M., and Buckel, W. (1995) *FEBS Lett.* **357,** 145–148
47. Rochet, J-C., and Bridger, W. A. (1994) *Protein Sci.* **3,** 975–981
48. Murzin, A. G., Brenner, S. E., Hubbard, T. and Chothia, C. (1995) *J. Mol. Biol.* **247,** 536–540
49. Hersch, L. B., and Jencks, W. P. (1967) *J. Biol. Chem.* **242,** 3468–3480

Crystallographic Trapping of the Glutamyl-CoA Thioester Intermediate of Family I CoA Transferases

Erumbi S. Rangarajan, Yunge Li, Eunice Ajamian, Pietro Iannuzzi, Stephanie D. Kernaghan, Marie E. Fraser, Miroslaw Cygler and Allan Matte

J. Biol. Chem. 2005, 280:42919-42928.
doi: 10.1074/jbc.M510522200 originally published online October 27, 2005
